

Report

Contrast-Enhanced In Vivo Imaging of Breast and Prostate Cancer Cells by MRI

Olga Rodriguez^{1,2,†}
Stanley Fricke^{1,3,†}
Christopher Chien^{1,2}
Luis Dettin²
John VanMeter⁴
Erik Shapiro⁵
Hai-Ning Dai³
Mathew Casimiro^{1,2}
Lilia Ileva³
John Dagata⁶
Michael D. Johnson^{1,2}
Michael P. Lisanti⁷
Alan Koretsky⁵
Chris Albanese^{1,2,*}

¹Lombardi Cancer Center; ²Department of Oncology; ³Department of Neuroscience and ⁴Department of Neurology; Georgetown University Medical Center; Washington, DC USA

⁵Laboratory of Functional Molecular Imaging; National Institutes of Health; Bethesda, Maryland USA

⁶National Institute of Standards and Technology; Gaithersburg, Maryland USA

⁷Departments of Molecular Pharmacology and Medicine; Albert Einstein College of Medicine; Bronx, New York USA

[†]These authors contributed equally to this work.

*Correspondence to: Chris Albanese; Department of Oncology; Lombardi Comprehensive Cancer Center; Georgetown University Medical Center; Washington, DC 20057 USA; Tel.: 202.687.3305; Email: albanese@georgetown.edu

Received 11/01/05; Accepted 11/04/05

Previously published online as a Cell Cycle E-publication:
<http://www.landesbioscience.com/journals/cc/abstract.php?id=2295>

KEY WORDS

MRI, breast cancer, prostate cancer, superparamagnetic, nanoparticle, fluorescence, xenograft

ACKNOWLEDGEMENTS

See page 119.

ABSTRACT

The development of effective cancer therapies has been hampered, in part, by the inability to noninvasively follow tumor progression from the initial cancerous lesion through to metastasis. We have previously shown that superparamagnetic iron oxide particles can be used as magnetic resonance imaging contrast agents to label embryonic, mesenchymal and hematopoietic stem cells in vivo. Improving the capacity to non-invasively image cancer progression is an appealing method that could be useful for assessing the efficacy of anticancer therapies. We have established that human prostate (LNCaP, DU145, PC3), rodent prostate (TRAMPC1, YPEN-1), human breast (MDA-MB-231) and mouse mammary (Myc/VEGF) cancer cell lines were readily labeled by fluorescent superparamagnetic sub-micron particles of iron oxide (MPIOs). The MPIOs were essentially inert with respect to cell proliferation and tumor formation. Fluorescence stereomicroscopy and three dimensional magnetic resonance imaging (MRI) determined that subcutaneous, intramuscular or orthotopically implanted labeled cancer cells could be imaged, in vivo, despite in some cases being undetectable by manual palpation. The MPIO-labeled cancer cells could also be imaged, in vivo, at least 6 weeks after implantation. The fluorescent MPIOs further allowed for the ex vivo identification of tumors cells from histological sections. This study demonstrates the feasibility of using fluorescent MPIOs in prostate and breast cancer cell lines as both a negative contrast agent for in vivo MRI as well as a fluorescent tumor marker for optical imaging in vivo and ex vivo.

INTRODUCTION

Each year in the United States alone, roughly 34,000 deaths result from metastatic prostate cancer while approximately 40,000 patients succumb to metastatic breast cancer. Cancer metastases are the result of individual cells or groups of cells leaving the primary tumor site and entering either the lymphatic system or the vasculature. These cancer cells become established at distant sites, thereby developing into additional tumors. Early detection of breast cancer by mammography and of prostate cancer through digital rectal exams has resulted in the ability to treat lesions earlier while the identification of biomarkers of cancer progression such as PSA for prostate cancer allows for the longitudinal assessment of cancer treatment. Once detected, the primary treatments for both cancers are chemical ablation of steroid hormone function and/or surgical removal of affected tissue. While initially successful, many patients experience relapse with cancer that is no longer responsive to steroid ablation and a significant proportion of these patients die as the result of cancer metastases. Metastatic cancers, especially micro-metastases that evade clinical detection, represent a serious health concern and a serious clinical problem since current curative therapies for metastatic prostate cancer, for example, are by and large ineffective.¹ Our inability to clinically inhibit the progression to malignancy and metastasis is due, in part to a lack of understanding of the transformation process as well as the lack of effective preclinical models that allow for the longitudinal measurement in vivo, of the efficacy of therapeutics.

The in vivo study of cancer metastasis at the cellular level has often relied on extensive serial sectioning of target organs in order to assess tumor burden.² More recently, several techniques have been developed to follow the growth and metastasis of cancer cells, in vivo. For example, fluorescently labeling cells enabled the imaging of the growth and metastasis of either xenograft tumors or tumors induced in genetically engineered mice by microscopy. Dual fluorescence imaging allowed for the delineation of tumor cells from the host vasculature,³ however these studies are limited in both image resolution and the depth of imaging penetration of and are performed with cells that are either stably selected for

expression of a fluorescent protein or transformed with a retrovirus bearing a fluorescent marker, techniques that can permanently affect the cells phenotype and genotype in ways that are not easily quantified. Optical bioluminescence imaging also involves the use of cells or tissues that are engineered to express luminescence enzymes. Images are obtained through cooled CCD luminometry following the minimally invasive in vivo administration of luminescence substrates, such as luciferin. Similar to fluorescence microscopic imaging, this optical imaging modality is limited in both image resolution and imaging depth, although both are enhanced as compared to fluorescence imaging. Optical imaging is also incapable, in certain applications, of performing whole body three-dimensional imaging.

Nuclear, three-dimensional animal imaging can be performed using positron emission tomography (PET) or single photon emission computed tomography (SPECT).⁴ Both of these imaging modalities require the synthesis of high energy, short lived, radiolabeled targeted molecular probes that deliver whole body images with spatial resolution that meets or exceeds that obtainable by optical methods. The need for radioactive tracers however places a radiation safety and exposure burden on these experiments and the rapid decay of the radioactive tracers limits the longitudinal study of metastasis at the cellular level.

Magnetic resonance imaging (MRI) provides the technological means of producing three dimensional images of cancers in a non-invasive, nonradioactive manner. For example, recent developments in the engineering and use of MRI and MR spectroscopy in humans have greatly aided in the noninvasive diagnosis and treatment of prostate⁵ and breast cancers.⁶ Considerable progress has also been made in the development of MR contrast enhancing techniques and reagents, especially for use in the neurosciences.⁷

Advances in the use of iron-containing contrast agents have greatly improved the imaging capabilities of MRI clinically, for example to identify areas of altered cell populations associated with lymphatic prostate cancer metastases.⁸ One important application of the iron oxide core contained within sub-micron particles of iron oxide (MPIOs) is to act as a negative contrast agent for magnetic resonance imaging and potentially for in vivo cell tracking.⁹ We and others have previously demonstrated that superparamagnetic iron nanoparticles are useful reagents to study the fate of labeled stem cells and stromal cells in animal models.¹⁰⁻¹³ We hypothesized that by using MPIO- labeled cancer cells, it may be possible to image breast or prostate xenografts in vivo and noninvasively. If feasible, this would allow for the further investigation into the mechanisms underlying cancer progression as well as to permit the imaging, in real-time, of the effectiveness of existing or future cancer therapies, in vivo.

In this study, we established that human and rodent prostate and breast cancer cell lines are readily labeled by fluorescently tagged superparamagnetic MPIOs. We further established that the MPIOs are inert with respect to cellular division and tumor formation, were passed along to daughter cells during mitosis and that labeled cancer cells and tumors were visible in vivo by MRI and by fluorescence microscopy. This technology will enable the rapid, noninvasive, optical imaging and high-resolution three dimensional magnetic imaging of human cancer xenografts, in vivo.

METHODS AND MATERIALS

Superparamagnetic iron particles. The superparamagnetic MPIOs (Bangs Laboratories, IN.) employed are divinyl benzene inert polymer microspheres with a stated average size 960 nm. The particles contain a magnetite iron oxide component (greater than 27%), and a

fluorescein-5-isothiocyanate analog (Cat # ME02F, L010212B) component within the polymer matrix, with a COOH- surface moiety.

Cell lines. Human (LNCaP, DU-145 PC3) mouse (TRAMP C1) and rat (YPEN-1 prostate endothelial cell line) prostate derived cell lines and the human breast cancer cell line, MDA-MD-231, are from the ATCC (Rockville, MD). The MYC/VEGF mouse mammary tumor cell line was derived from a spontaneous tumor arising on an MMTV-c-Myc x MMTV-VEGF double transgenic mouse¹⁴ (here after referred to as Myc/VEGF). The LNCaP androgen-responsive human prostate adenocarcinoma cell line contains a mutant androgen receptor and is androgen sensitive, the DU-145 cell line and the PC3 cell line are AR negative, androgen-insensitive human prostate cancer cell lines. MDA-MD-231 human breast cancer cells are estrogen receptor (ER) negative and are estrogen insensitive. All cell lines can be grown as xenografts in nude mice. LNCaP cells were cultured in RPMI with 10% FCS plus 10 nM dihydrotestosterone (DHT), DU145 and PC3 cells do not require DHT. TRAMP C1 cells were derived from TRAMP mice,¹⁵ are tumorigenic in C57/BL6 mice, and are maintained in DMEM, 4 mM L-glutamine, 1.5 g/L sodium bicarbonate 4.5 g/L glucose supplemented with 0.005 mg/ml bovine insulin and 10 nM DHT, 5% fetal bovine serum, 5%; Nu-Serum IV. YPEN-1 cells were derived from rat prostate vascular endothelial cells and were grown in DMEM, 2 mM L-glutamine, 1.5 g/L sodium bicarbonate, 0.1 mM non-essential amino acids, 1.0 mM sodium pyruvate, 0.03 mg/ml heparin and 5% fetal bovine serum.

MPIO labeling of cells. Cells were incubated overnight with MPIOs (1 x 10⁹ particles in 10 ml media), washed three times with vigorous shaking to remove free particles, trypsinized and resuspended in culture media. Density centri-fugation by Ficoll-paque (Amersham, Biosciences) was carried out as necessary in 15 ml Falcon tubes by layering 1–4 million cells in 3 ml of media on top of Ficoll. Cells were spun for 30 minutes at 400x G. Most free particles pelleted, leaving a layer of cells at the interface of the two layers. Cells were washed twice with 10 mls of media, pelleted and replaced in culture media.¹¹

Flow cytometry. Cell cycle analysis was performed on MPIO-labeled and unlabeled cells using a Becton Dickinson FACStar Plus dual laser fluorescence activated cell sorting (FACS) machine. Analyses were performed after 24 to 72 hours in culture following labeling. Cells were trypsinized and fixed in 10% methanol and resuspended in PBS containing 20 mg/ml propidium iodide (PI) and RNase A (5 units). The cells were subjected to cell cycle analysis and sub-G₁ content determination (a measure of DNA fragmentation) as previously described.¹⁶

Atomic force microscopy. Atomic Force Microscopy (AFM) was performed on aliquots of the 960 nm MPIOs. The particles were diluted in deionized water and were micropipetted onto an ultrasonically cleaned silicon substrate with either a native oxide or a poly-L lysine coating. Imaging was performed using a Veeco MultiMode microscope with a Nanoscope IV controller. Topography by tapping mode with Q control [RTESP cantilevers of ~ 320–360 kHz and k ~ 20–60 N/m], phase imaging, and magnetic force microscopy using magnetic coated tips [MESP 68 kHz] was performed in lift mode.

Fluorescence microscopy. Confocal fluorescence microscopy was carried out on an Olympus IX-70 Laser Confocal Microscope. Fluorescence stereomicroscopy was performed on a Nikon SMZ-1500 EPI-Fluorescence Stereoscope System.

Electron microscopy. Cells growing in 12 well plate, 96 hours after cell labeling, were fixed in phosphate buffered 2% paraformaldehyde, 2.5% glutaraldehyde mixture, washed five times, 5 min each in 1 x PBS, post fixed with 1% OsO₄ for 20 min and washed with dH₂O. The fixed cells were then stained with 2% uranyl acetate, washed in dH₂O, dehydrated in graded alcohols (50, 70, 95, 95, 100, 100%), embedded in SPURR embedding solution and sectioned using a PowerTome XL ultramicrotome at ~70 nm (gold interference color). Sections, mounted in 300 mesh copper grids, were post-stained with uranyl acetate and lead citrate and visualized on a Hitachi H-7600 high-resolution Transmission Electron Microscope (TEM).

Preparation of animals for MRI. All procedures were carried out in accordance with Georgetown University Animal Use Committee approval. The protocols met all recommendations of the Animal Welfare Act, the

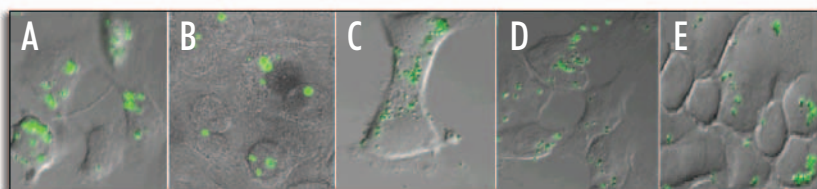


Figure 1. In vitro cell labeling. Confocal images of MPIO-labeled (A) DU145, (B) PC3, (C) TRAMPC1, (D) MDA-MB-231 and (E) Myc/VEGF cancer cells.

acid (V:V) and 5% potassium ferrocyanide (W:V) for 30 minutes, and rinsed in distilled water. The slides were counterstained for five minutes in nuclear Fast Red, washed in distilled water, dehydrated and mounted. Immunohistochemical staining for epithelial cytokeratins was performed using a pan-cytokeratin antibody (Dako, A0575) and a horseradish peroxidase conjugated secondary antibody. Following exposure to the chromogen, diaminobenzidine, the slides were counterstained with H&E.

RESULTS

Superparamagnetic labeling of human and rodent cancer cell lines.

In order to establish the feasibility of imaging cancer cells on an individual basis, cell labeling experiments were carried out using superparamagnetic MPIOs of approximately 960 nanometers (nm) in human and mouse prostate epithelial cell lines, a rat prostate endothelial cell line and a human breast cancer cell line. Following overnight incubation with the MPIOs, the cells were either purified by density gradient separation or used directly. Cells were imaged by fluorescence microscopy three days after labeling to determine if the MPIOs had been internalized. Multiple particles were observed in the cytoplasmic compartment of DU145 (Fig. 1A) and PC3 (Fig. 1B) human prostate cancer cell lines, TRAMPC1 mouse prostate cancer cell line (Fig. 1C), MDA-MD-231 human breast cancer cells (Fig. 1D) and the Myc/VEGF mouse mammary tumor cell line (Fig. 1E). Similar results were seen with LNCaP prostate cancer cells and YPEN-1 rat prostate endothelial cells (not shown) although the YPEN-1 cells exhibited a diminished capacity for MPIO uptake and had to be purified away from unincorporated particles by gradient centrifugation. The internalized MPIOs appeared functionally inert as no change in cell attachment or initial viability was observed. Additionally, the internalized MPIOs were efficiently transmitted to the daughter cells during cellular division as seen in the TRAMPC1 cells (Fig. 1C).

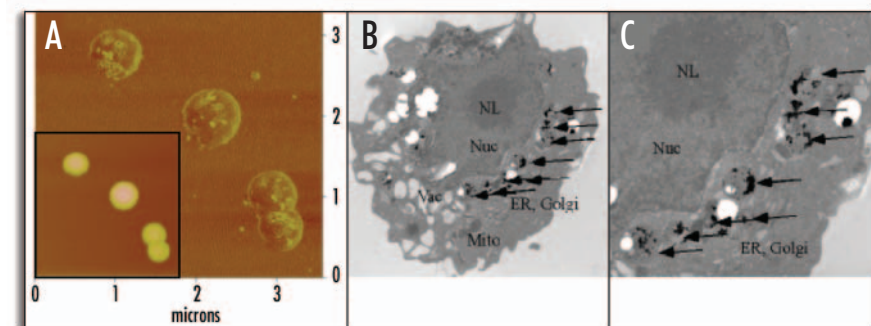


Figure 2. MPIO imaging. (A) Atomic Force Microscopy of MPIOs using phase imaging in tapping mode with enhanced Q-control. Inset: Simultaneously obtained AFM topographic image. (B) Electron micrograph (4000X) of DU145 prostate cancer cells labeled with MPIOs. (C) EM at 8000X (final magnification). Arrows indicate MPIOs, Black areas represent the inhomogeneous iron component. NL, nucleolus, Nuc, nucleus, Mito, mitochondria, ER, endoplasmic reticulum.

Guide for the Care and Use of Laboratory Animals as stated in the NIH guide and the UKCCCR guidelines. Animals to be imaged were anesthetized and placed in our proprietary, in-house designed, animal management system,¹⁷ specifically modified for mouse prostate imaging. Animals were anesthetized which was maintained during imaging with 1.5% isoflurane.

Tumorigenicity in mice. Xenograft injections of cancer cells were carried out in 6–8 week old Ncr-nu athymic nude mice or in FVB-N mice as previously described.¹⁸ Animals were injected with at least 1×10^6 labeled or unlabeled tumor cells. Cell growth was monitored both by manual palpation and by MRI. Tumors were excised at autopsy and were either frozen or fixed for histology. Cancer cells were injected either intramuscularly or subcutaneously or were orthotopically implanted within the mammary fat pad. All xenograft/allograft experiments were carried out on at least two separate occasions using freshly prepared labeled cell preparations.

MRI. Imaging was performed on the Bruker 7.0 tesla spectrometer/imager horizontal 20 cm bore magnet running Paravision 2.1 software. The magnet was equipped with 100 gauss/cm microimaging gradients and a 72 mm proton microimaging birdcage volume coil. Whole body three dimensional MRI data sets were collected using a T2*-weighted GEFI gradient echo imaging sequences, Matrix = $256 \times 256 \times 256$, TE = 4 ms, TR = 70 ms, Flip angle, 30°, as previously described.¹¹ Image resolution was approximately $100 \mu\text{m} \times 100 \mu\text{m} \times 300 \mu\text{m}$. For imaging of mice, the animals were placed in a custom made animal holding device under continuous isoflurane anesthesia. Physiological monitoring of body temperature was achieved with a Luxtron fiber optic thermometer and body temperature was maintained with a warm water blanket at 37°C. All in vivo experiments were carried out on at least two separate occasions.

Tissue sectioning and histology. Recovery of the labeled and unlabeled tumors was performed at autopsy. Tumor and tissue specimens were either frozen in embedding compound (OCT, Tissue-Tek) or fixed in neutral buffered formalin. Paraffin embedded or frozen specimens were sectioned (5–10 micron thickness) and stained with hematoxylin and eosin (H&E) or processed for fluorescent microscopy. Prussian Blue (Perl) staining was performed on paraffin embedded tissue specimens using an acidic potassium ferrocyanide solution. Briefly, paraffin sectioned samples were deparaffinized and rehydrated. The slides were stained in a mixture of 10% hydrochloric

cell line (Fig. 1E). Similar results were seen with LNCaP prostate cancer cells and YPEN-1 rat prostate endothelial cells (not shown) although the YPEN-1 cells exhibited a diminished capacity for MPIO uptake and had to be purified away from unincorporated particles by gradient centrifugation. The internalized MPIOs appeared functionally inert as no change in cell attachment or initial viability was observed. Additionally, the internalized MPIOs were efficiently transmitted to the daughter cells during cellular division as seen in the TRAMPC1 cells (Fig. 1C).

In order to establish that the incorporated MPIOs are stable over time, the cells were cultured for an additional five days and reimaged. Since the particles were passed to the daughter cell during mitosis, many cells still contained the fluorescent superparamagnetic MPIOs in varying quantities (not shown).

Imaging of superparamagnetic MPIOs. The particle size and subcellular localization was established using either an atomic force microscope (AFM) or a transmission electron microscope (TEM). Isolated MPIOs and particle aggregates were observed in solution using the AFM (Fig. 2A). The size of the individual MPIOs ranged from approximately 650 nm to 900 nm. Inhomogeneous distribution of the iron oxide-containing magnetite within individual MPIOs is clearly revealed by AFM phase images. Phase imaging senses local hardness variations and therefore enhances contrast between iron oxide (bright in the phase image), relative to the polymer matrix of the MPIO. In order to establish the subcellular localization of the MPIOs, labeled PC3 cells were subjected to TEM four days after incubation with the MPIOs. As seen in Figure 2B and C, the MPIOs were visible within the cytoplasmic compartment, were perinuclear and were located in intracellular organelles, possibly endosomes. The average size of the MPIOs observed by TEM was approximately 850 nm, similar to that observed by AFM.

Cell cycle analysis. We had previously demonstrated that the labeling of primary hematopoietic or mesenchymal stem cells with MPIOs had no profound impact on cellular proliferation and lineage differentiation,¹¹ however, the growth characteristics following particle labeling of transformed cancer cell lines had not been tested. MDA-MB-231, Myc/VEGF and TRAMPC1 cells (Fig. 3) and DU145 and PC3 cells (not shown) were labeled with 1×10^9 particles per 10 ml culture media for 24 to 72 hours. Cell cycle analyses were performed by FACS, using unlabeled cells as controls.

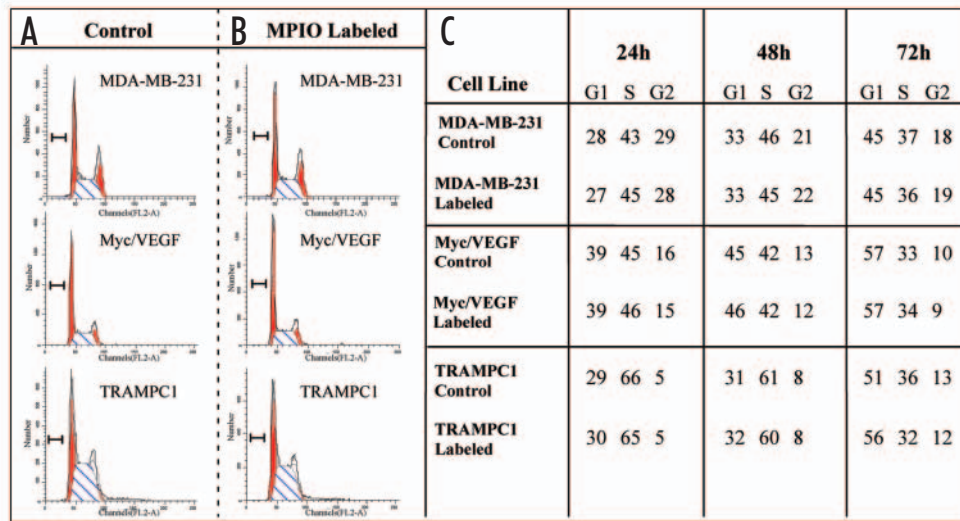


Figure 3. Intracellular MPIOs are inert in cancer cells. Breast and prostate cancer cell lines were analyzed by flow cytometry for changes in cell cycle progression. Representative cell cycle profiles at 48 hrs of (A) control and (B) MPIO-labeled cells. (C) Cell cycle profile of both control and MPIO-labeled cells at 24, 48 and 72 hrs. Values are shown as percent of total cells. The bars in (A and B) denote the sub-G₁ population of apoptotic cells.

The cell cycle profile on the labeled cancer cells revealed that there was no difference in the cell cycle profile of the labeled versus nonlabeled cells. The lack of a sub G₁ cell cycle fraction, a measure of late-stage apoptosis brought about by DNA fragmentation¹⁶ (shown as bars in Fig. 3A and B), suggested that the MPIOs had little effect on apoptosis.

MRI in vitro. To establish the parameters required for visualization by magnetic resonance imaging, the MPIOs were initially suspended in tissue culture media-containing soft agarose and layered in a glass NMR tubes alongside soft agarose alone. As seen in Figure 4A, the MPIOs in suspension were clearly visible by the T2* sequence, as previously described.¹¹ Next, this method was applied to MPIO-labeled DU145 prostate cancer cells that had been resuspended in tissue culture media-containing soft agarose. As is shown in Figure 4C, the MPIOs produced a profound negative contrast under T2* imaging, allowing the cancer cells to be detected by MRI. The beads were also placed in an ‘X’ arrangement on agarose and imaged by fluorescence microscopy (Fig. 4D) and by T2* MRI (Fig. 4E).

MRI of MPIO-labeled prostate cancer cells in vivo. To determine the extent to which small xenograft tumors could be imaged, one million TRAMPC1 cells were injected subcutaneously in the flank of male Ncr-nu athymic nude mice and allowed to establish. Serial three dimensional image datasets were collected on anesthetized mice using T2* MR imaging sequences 3- to 6-weeks post-implantation. All xenograft experiments were performed on multiple mice with similar results and representative data are shown. Labeled TRAMPC1 prostate cancer cells (Fig. 5A, arrow) were visible as a negative contrasted image, versus unlabeled cells (Fig. 5B). To confirm that the MPIOs were intracellular and that the negative contrast correlated with the presence of the MPIOs, the tumors were excised, serially sectioned and imaged by microscopy. Figure 5C shows that extensive fluorescence was seen within the labeled, but not unlabeled, tumor (Fig. 5D). Paraffin embedded histological tissue sections from the tumor were also stained for iron using Perl’s Prussian blue. Areas of intensely blue stained cells, demonstrating the presence of the iron MPIOs within the tumor cells, were visible (Fig. 5E) among cells negative for iron staining (Fig. 5F). Immunohistochemical staining for epithelial cytokeratins confirmed that the MPIO-labeled cells were prostate cancer cells (not shown). The number of labeled cells and the average number of MPIO’s per labeled cell was determined within the tumor. Within 0.7 mm from the tumor core (the injection site), 90% (± 4 S.D. (standard Deviation)) of the cells were labeled with an average of 13 (± 3 S.D.) MPIOs per cell. The average number of labeled cells declined to 65% (± 10% S.D.) with 4.5 (± 2.9 S.D.) MPIOs per cell at 0.7 mm to 1.6 mm from the injection site. The cells appeared as unlabeled by 4 mm from the injection site. Approximately 500 cells were analyzed in each set.

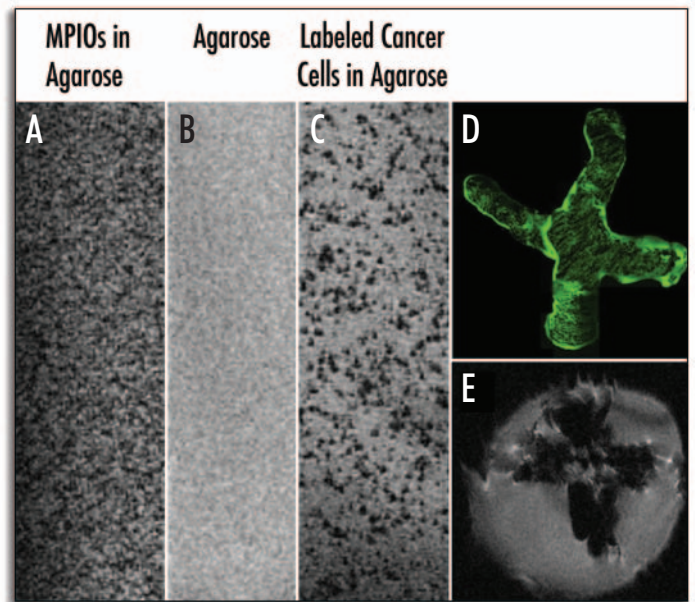


Figure 4. Imaging of MPIOs. T2* MRI of (A) MPIOs in an agarose suspension, (B) Agarose alone. (C) Labeled DU145 cells in an agarose suspension. (D) Fluorescence image of MPIOs on an agarose plug, (E) T2* image of MPIOs from (D).

MRI of MPIO-labeled breast cancer cells in vivo. The MDA-MB-231 human breast cancer cell line is an estrogen-independent, estrogen receptor negative cell line that has been shown to be tumorigenic in immunocompromised mice.¹⁹ To investigate if the MPIOs affected ectopic tumor formation, MDA-MB-231 cells were labeled with MPIOs and implanted in the hind limb of female Ncr-nu athymic nude mice via intramuscular injection. Unlabeled MDA-MB-231 cells were implanted in the contralateral leg muscle. MRI and fluorescence stereomicroscopy were performed three weeks post-implantation. The labeled breast cancer cells are clearly visible within the muscle by both imaging methods (Figs. 6A and D). The MPIOs were also visible within H&E stained histological sections (Fig. 6E) and Perl’s staining further confirmed the presence of the MPIOs within the cells (Fig. 6F). Furthermore, the labeled cells extended outwards from the point

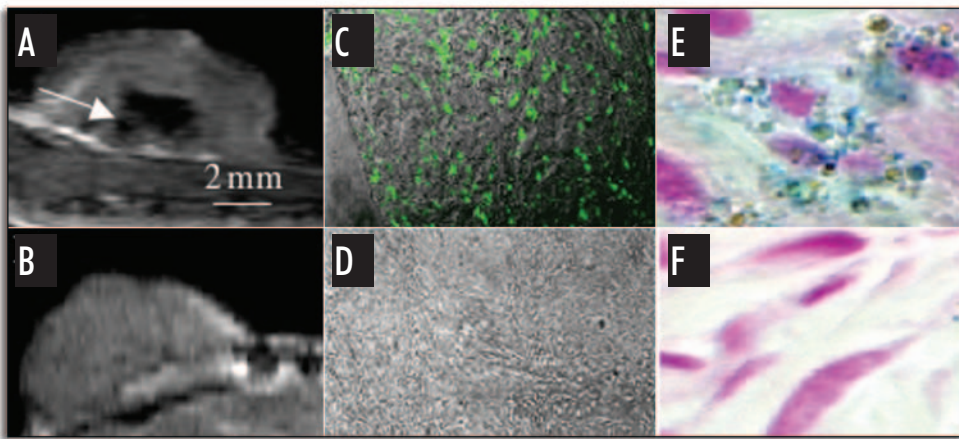


Figure 5. Imaging of mouse prostate cancer xenografts. MPIO-labeled (A) and unlabeled (B) TRAMP-C1 mouse prostate xenografts were imaged in vivo by T2*-weighted MRI. (C and D) Frozen tumor sections imaged by confocal fluorescent microscopy. Perl's Prussian blue staining of MPIO positive cells (E) or MPIO negative cells (F). The arrow in (A) identifies the negative contrast MR image created by the superparamagnetic MPIOs.

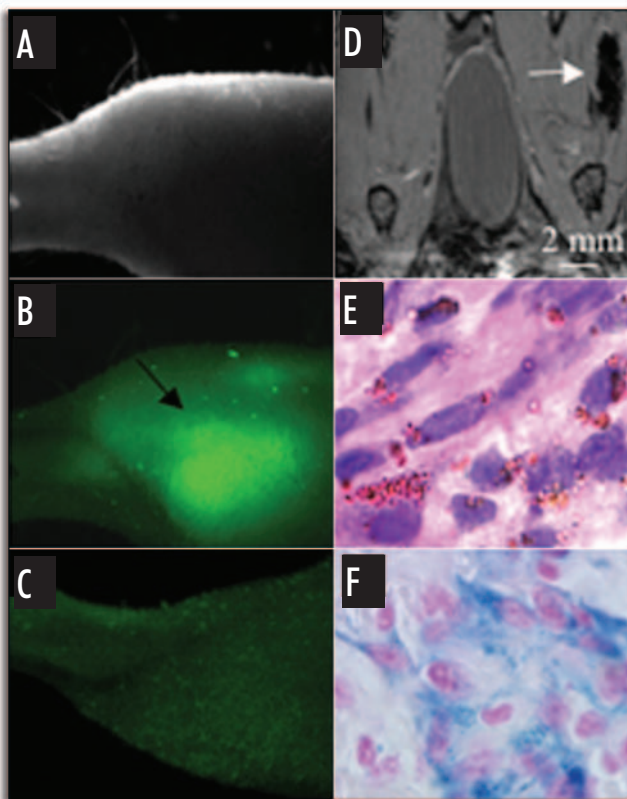


Figure 6. Ectopic breast tumor imaging. MPIO-labeled (A,B) or unlabeled (C) MDA-MB-231 cells were injected intramuscularly and imaged. MPIO-labeled tumors were identified by fluorescence stereomicroscopy (B), as opposed to the contralateral unlabeled tumor (C). Coronal MRI section (D) showing labeled intramuscular tumor cells (arrow). Confocal microscopy (E) and Perl's Prussian blue staining (F) of the excised particle-labeled tumor.

of initial injection, as was seen using the TRAMP-C1 cells (not shown). Immunohistochemical staining for cytokeratins verified that the particle-labeled cells were breast epithelial cells (not shown). In a separate series of experiments, the effect of MPIO labeling on estrogen independent growth was investigated. Labeled and unlabeled MDA-MB-231 cells were implanted in the inguinal fatpad area of male Ncr-nu athymic nude mice.

Tumors that formed were imaged by fluorescence stereomicroscopy, MRI and confocal microscopy. As was seen with the intramuscular implantation experiments, the labeled tumor cells were visible (Fig. 7), immunohistochemical staining for cytokeratin again confirmed that the MPIO-positive cells were breast cancer cells (Fig. 7D). TEM confirmed that the particles were intracellular (Fig. 7E and F).

MRI of MPIO-labeled mouse mammary cancer cells in vivo. To test the ability of MRI to image orthotopic mammary tumors in immune-competent mice, allograft experiments were carried out with labeled and unlabeled Myc/VEGF mouse mammary cancer cells implanted in the inguinal mammary fat pad of syngeneic female FVBN mice. The labeled mammary tumor cells were visible by both MRI and fluorescence stereomicroscopy, in vivo (Fig. 8A and B). Subsequent confocal fluorescence imaging on frozen sections of the excised tissue confirmed that these cells contained MPIOs (Fig. 8C). The MPIOs were also seen in histological sections (Fig. 8D). Additionally, immunohistochemical staining for cytokeratin confirmed that the cells containing the MPIOs were mammary tumor cells (Fig. 8E and F).

DISCUSSION

Our data establishes that MPIOs can be employed to label, and thereby visualize, breast and prostate cancer xenografts using both magnetic and optical imaging modalities. We have shown that a variety of mouse, human and rat cell lines can be effectively labeled in vitro with commercially available polymer embedded superparamagnetic MPIOs. The MPIOs, which are also fluorescently labeled, are internalized within hours of administration without the need for liposomes, targeting moieties or other reagents to enhance uptake. We also demonstrate that the superparamagnetic MPIOs are functionally inert with respect to cellular division, tumor xenograft formation or steroid hormone independence. Since the particles are transmitted to daughter cells, further expansion in the quantity of contrast-labeled cells occurs. These results are in agreement with our previous studies, where (A) hematopoietic stem cells and mesenchymal stem cells labeled with these particles retained both their proliferative function as well as capacity to undergo differentiation¹¹ and (B) single cell mouse embryos develop normally following injection with the MPIOs with individual labeled cells visible in embryos to day 11.5.¹⁰ Our previous experiments using primary rodent mesenchymal stem cells required the removal of unincorporated MPIOs by Ficoll density centrifugation, which resulted in a slight enhancement of cellular proliferation.¹¹ Unlike our previous experiments, the transformed prostate and mammary epithelial cells avidly incorporated the MPIOs, with few unincorporated MPIOs observed following 12 hours of addition and no indication of altered proliferation. We did notice, however, a decrease in the efficiency of cell labeling with larger (> 3 μm) particles (OR and CA, data not shown), suggesting this may be nearing a physiological size limit for internalization. Also, the efficiency of incorporation of the MPIOs was reduced in YPEN-1 rat prostate endothelial cells as compared with breast or prostate epithelial cells. The reason for the differences in efficiency between the epithelial cells and the endothelial cells is not presently known. The efficiency of uptake in YPEN-1 cells may

be enhanced with the use of a lipofection reagent,²⁰ possibly negating the need for Ficoll gradient purification.

Stable fluorescent (e.g., RFP, GFP) labeling of cells has enabled the *in vivo* optical imaging of tumors and metastases in two dimensions.^{21,22} Optical two-dimensional imaging has been used to visualize PC3 (prostate)²³ and MDA-MB-231 (breast)²⁴ cancer xenograft metastases using *in vivo* bioluminescence imaging (BLI). Left ventricle intracardiac injection of cancer cells that had been retrovirally transduced with luciferase reporter system resulted in highly metastatic subpopulations of MDA-MB-231 cells which could be selected by fluorescence activated cell sorting, and the transcriptosomal profile of metastasis-related genes investigated by microarray and PCR.²⁴ Our three-dimensional magnetic resonance images of the MPIO-labeled cells enabled the identification of both the labeled cells as well as the anatomical structure of the animal using a single imaging modality. We have also shown that the MPIOs could also be used to generate optical fluorescence images, without the need for extensive *in vitro* antibiotic selection or viral infection of the target cell line. Since MPIO labeled cancer cells contain at least one iron particle, populations of cells could theoretically be rapidly selected from tissues, blood or the lymphatic system through the use of a magnetic field or by FACS. It is also not inconceivable that the MPIOs could be reengineered to carry other markers, such as quantum dots, radio-tracers or even enzymes.

The ability to visualize the growth and dissemination of cancer cells *in vivo* would represent a potentially powerful technology in the development of effective cancer therapies. In human patients for example, androgen-independent prostate cancer metastases represent a serious clinical problem and a severe health risk. While the current chemotherapies can be effective in palliative care,²⁵ and despite intensive research and extensive clinical trials, no known curative agent or regimes currently exist. Similarly, treatment of high-risk breast cancers (e.g., ER-negative, ErbB-2++ cancers) with lymph node metastases results in a poor outcome even following dosage intensive chemotherapies.²⁶ An engineered colloidal superparamagnetic nanoparticle (feruglose) showed promise as a contrast agent for preoperative breast tumor grading through imaging of the tumor microvasculature²⁷ *in vivo*, and engineered nanoparticles that targeted lymph node compartments proved useful in identifying nodal prostate metastases by MRI, by virtue of a tumor-associated loss of negative contrast normally generated by properly targeted nanoparticles.⁸ Dextran coated iron-labeled embryonic stem cells could be tracked over time by MR in animal models of traumatic brain and spinal injury¹³ as well as in humans.²⁸ Engineered crosslinked crystals of iron oxide (CLIOs)²⁹ were able to target gliosarcoma³⁰ and endothelial³¹ cells among others³² *in vivo* and MRI has been used to visualize mouse tumors using iron oxide-labeled, tumor-targeted NK cells.³³ Our data further supports the hypothesis that individual cells or populations of breast and prostate cancer cells, labeled with the fluorescent MPIOs can be imaged longitudinally by negative contrast MRI, *in vivo*. Given the importance of human xenograft⁴ and mouse allograft studies in the current paradigm of drug development and the capacity to establish cell lines that mimic alterations found in human epithelial cancers, our data suggests that the efficacy of

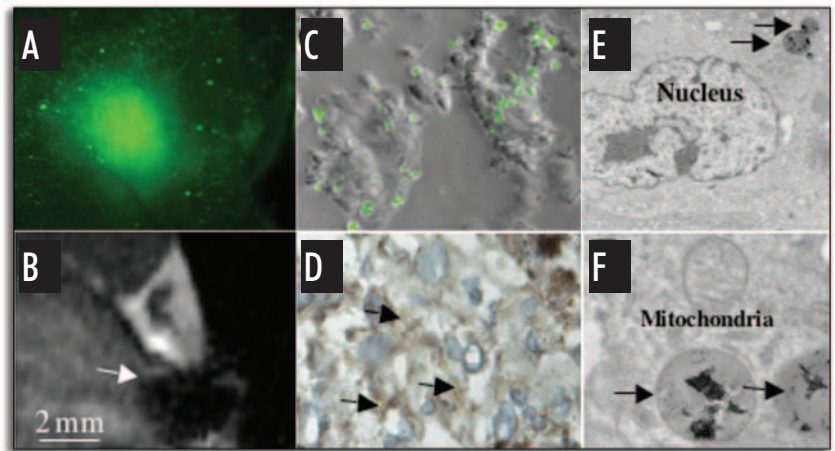


Figure 7. Estrogen-independent, orthotopic breast tumor imaging. (A) fluorescence stereomicroscopy and (B) MRI of labeled MDA-MB-231 cells implanted in the inguinal area corresponding to the mammary fat pad. (C) Confocal fluorescence microscopy and (D) immunohistochemical staining for cytokeratin (brown). (E and F) Electron micrograph of intracellular MPIOs. Arrowheads in (B) indicate negatively-contrasted tumor. Arrows in (D-F) identify representative intracellular MPIOs.

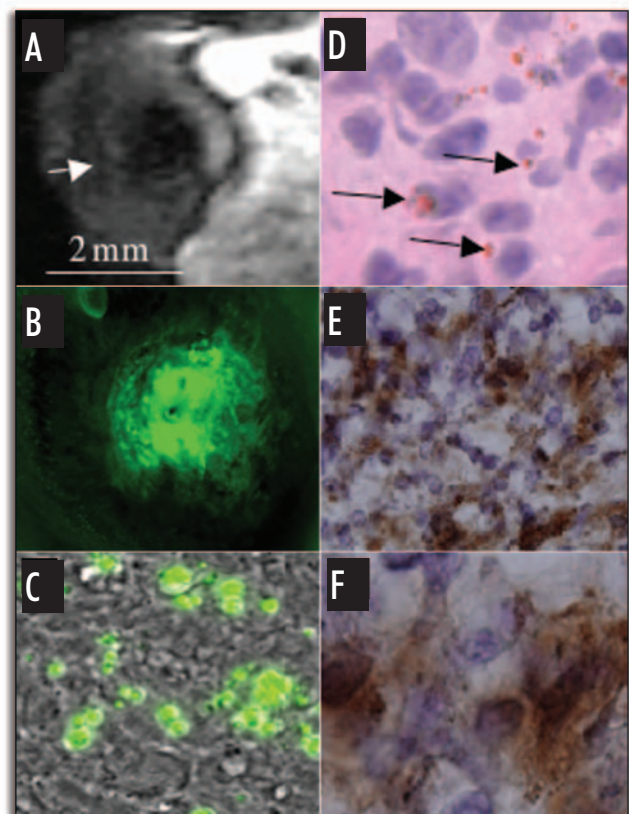


Figure 8. Myc/VEGF mouse mammary isograft imaging in syngenic FVBN mice. (A) MRI of labeled Myc/VEGF mammary tumor. (B) Stereo fluorescence image of mammary xenograft. (C) Confocal fluorescence microscopy. (D) H&E staining and (E and F) immunohistochemical staining for cytokeratin (brown) of Myc/VEGF xenograft. Arrows, identify representative MPIOs.

virtually any given cancer therapeutic could be rapidly and reproducibly investigated using a variety of human and mouse cell lines in non-invasive preclinical trials using the MPIOs. Additional modification of the iron oxide nanoparticles, similar to that performed on CLIOs, may in the future enable their localization to established epithelial tumors, *in vivo*.

Acknowledgements

This work was supported in part by ACS IRG 97-152 and R03CA20337 and U54 CA100970-02 (C.A.) and by the Lombardi Comprehensive Cancer Center Microscopy and Imaging Shared Resource, the Lombardi Comprehensive Cancer Center Histopathology and Tissue Shared Resource, U.S. Public Health Service Grant 2P30-CA-51008 and 1S10 RR15768-01. O.R. was funded by the Lombardi Comprehensive Cancer Centers NCI Tumor Cell Biology postdoctoral training grant, NCI-CA09686T32. Drs. Koretsky and Shapiro were supported by the NINDS, NIH intramural research program. Disclaimer: Certain brands of commercial equipment are identified in this article. Such descriptions do not imply recommendations or endorsements by NIST, nor does it imply that the equipment identified is necessarily the best available for the purpose.

References

- Feldman BJ, Feldman D. The development of androgen-independent prostate cancer. *Nat Rev Cancer* 2001; 1:34-45.
- Bouzahzah B, Albanese C, Ahmed F, Pixley F, Lisanti MP, Segall JD, Condeelis J, Joyce D, Minden A, Der CJ, Chan A, Symons M, Pestell RG. Rho family GTPases regulate mammary epithelium cell growth and metastasis through distinguishable pathways. *Mol Med* 2001; 7:816-30.
- Yang M, Reynoso J, Jiang P, Li L, Moossa AR, Hoffman RM. Transgenic nude mouse with ubiquitous green fluorescent protein expression as a host for human tumors. *Cancer Res* 2004; 64:8651-6.
- Albanese C, Rodriguez O, Johnson MD, Fricke S. Models of prostate cancer. *Drug Discovery Today: Disease Models* 2005; 2:7-13.
- Zakian KL, Eberhardt S, Hricak H, Shukla-Dave A, Kleinman S, Muruganandham M, Sircar K, Kattan MW, Reuter VE, Scardino PT, Koutcher JA. Transition zone prostate cancer: Metabolic characteristics at 1H MR spectroscopic imaging—initial results. *Radiology* 2003; 229:241-7.
- Partridge SC, Gibbs JE, Lu Y, Esserman LJ, Tripathy D, Wolverson DS, Rugo HS, Hwang ES, Ewing CA, Hylton NM. MRI measurements of breast tumor volume predict response to neoadjuvant chemotherapy and recurrence-free survival. *AJR Am J Roentgenol* 2005; 184:1774-81.
- Jasanoff A. Functional MRI using molecular imaging agents. *Trends Neurosci* 2005; 28:120-6.
- Harisinghani MG, Barentsz J, Hahn PF, Deserno WM, Tabatabaei S, van de Kaa CH, de la Rosette J, Weissleder R. Noninvasive detection of clinically occult lymph-node metastases in prostate cancer. *N Engl J Med* 2003; 348:2491-9.
- Shapiro EM, Skrtic S, Koretsky AP. Sizing it up: Cellular MRI using micron-sized iron oxide particles. *Magn Reson Med* 2005; 53:329-38.
- Shapiro EM, Skrtic S, Sharer K, Hill JM, Dunbar CE, Koretsky AP. MRI detection of single particles for cellular imaging. *Proc Natl Acad Sci USA* 2004; 101:10901-6.
- Hinds KA, Hill JM, Shapiro EM, Laukkanen MO, Silva AC, Combs CA, Varney TR, Balaban RS, Koretsky AP, Dunbar CE. Highly efficient endosomal labeling of progenitor and stem cells with large magnetic particles allows magnetic resonance imaging of single cells. *Blood* 2003; 102:867-72.
- Sykova E, Jendelova P. Magnetic resonance tracking of implanted adult and embryonic stem cells in injured brain and spinal cord. *Ann NY Acad Sci* 2005; 1049:146-160.
- Jendelova P, Herynek V, Urdzikova L, Glogarova K, Kroupova J, Andersson B, Bryja V, Burian M, Hajek M, Sykova E. Magnetic resonance tracking of transplanted bone marrow and embryonic stem cells labeled by iron oxide nanoparticles in rat brain and spinal cord. *J Neurosci Res* 2004; 76:232-43.
- Pei XF, Noble MS, Davoli MA, Rosfjord E, Tilli MT, Furth PA, Russell R, Johnson MD, Dickson RB. Explant-cell culture of primary mammary tumors from *MMTV-c-Myc* transgenic mice. *In Vitro Cell Dev Biol Anim* 2004; 40:14-21.
- Greenberg NM, DeMayo F, Finegold MJ, Medina D, Tilley WD, Aspinall JO, Cunha GR, Donjacour AA, Matusik RJ, Rosen JM. Prostate cancer in a transgenic mouse. *Proc Natl Acad Sci USA* 1995; 92:3439-43.
- Albanese C, D'Amico M, Reutens AT, Fu M, Watanabe G, Lee RJ, Kitsis RN, Henglein B, Avantaggiati M, Somasundaram K, Thimmapaya B, Pestell RG. Activation of the *cyclin D1* gene by the E1A-associated protein p300 through AP-1 inhibits cellular apoptosis. *J Biol Chem* 1999; 274:34186-95.
- Fricke ST, Vink R, Chiodo C, Cernak I, Ileva L, Faden AI. Consistent and reproducible slice selection in rodent brain using a novel stereotaxic device for MRI. *J Neurosci Methods* 2004; 136:99-102.
- Lee RJ, Albanese C, Fu M, D'Amico M, Lin B, Watanabe G, Haines IIIrd GK, Siegel PM, Hung MC, Yarden Y, Horowitz JM, Muller WJ, Pestell RG. *Cyclin D1* is required for transformation by activated Neu and is induced through an E2F-dependent signaling pathway. *Mol Cell Biol* 2000; 20:672-83.
- Zugmaier G, Ennis BW, Deschauer B, Katz D, Knabbe C, Wilding G, Daly P, Lippman ME, Dickson RB. Transforming growth factors type beta 1 and beta 2 are equipotent growth inhibitors of human breast cancer cell lines. *J Cell Physiol* 1989; 141:353-61.
- Matuszewski L, Persigehl T, Wall A, Schwindt W, Tombach B, Fobker M, Poremba C, Ebert W, Heindel W, Bremer C. Cell tagging with clinically approved iron oxides: Feasibility and effect of lipofection, particle size, and surface coating on labeling efficiency. *Radiology* 2005; 235:155-61.
- Yang CS, Vitto MJ, Busby SA, Garcia BA, Kesler CT, Gioeli D, Shabanowitz J, Hunt DF, Rundell K, Brautigan DL, Paschal BM. Simian virus 40 small t antigen mediates conformation-dependent transfer of protein phosphatase 2A onto the androgen receptor. *Mol Cell Biol* 2005; 25:1298-308.
- Burton DW, Geller J, Yang M, Jiang P, Barken I, Hastings RH, Hoffman RM, Deftos LJ. Monitoring of skeletal progression of prostate cancer by GFP imaging, X-ray, and serum OPG and PTHrP. *Prostate* 2005; 62:275-81.
- Schneider A, Kalikin LM, Mattos AC, Keller ET, Allen MJ, Pienta KJ, McCauley LK. Bone turnover mediates preferential localization of prostate cancer in the skeleton. *Endocrinology* 2005; 146:1727-36.
- Minn AJ, Kang Y, Serganova I, Gupta GB, Giri DD, Doubrovin M, Ponomarev V, Gerald WL, Blasberg R, Massague J. Distinct organ-specific metastatic potential of individual breast cancer cells and primary tumors. *J Clin Invest* 2005; 115:44-55.
- Kasamon KM, Dawson NA. Update on hormone-refractory prostate cancer. *Curr Opin Urol* 2004; 14:185-93.
- Somlo G, Frankel P, Chow W, Leong L, Margolin K, Morgan Jr R, Shibata S, Chu P, Forman S, Lim D, Twardowski P, Weitzel J, Alvarnas J, Kogut N, Schriber J, Fermin E, Yen Y, Damon L, Doroshow JH. Prognostic indicators and survival in patients with stage IIIB inflammatory breast carcinoma after dose-intense chemotherapy. *J Clin Oncol* 2004; 22:1839-48.
- Daldrup-Link HE, Kaiser A, Helbich T, Werner M, Bjornerud A, Link TM, Rummeny EJ. Macromolecular contrast medium (feruglose) versus small molecular contrast medium (gadopentetate) enhanced magnetic resonance imaging: Differentiation of benign and malignant breast lesions. *Acad Radiol* 2003; 10:1237-46.
- Neuwelt EA, Varallyay P, Bago AG, Muldoon LL, Nesbit G, Nixon R. Imaging of iron oxide nanoparticles by MR and light microscopy in patients with malignant brain tumours. *Neuropathol Appl Neurobiol* 2004; 30:456-71.
- Josephson L, Kircher MF, Mahmood U, Tang Y, Weissleder R. Near-infrared fluorescent nanoparticles as combined MR/optical imaging probes. *Bioconjug Chem* 2002; 13:554-60.
- Kircher MF, Allport JR, Graves EE, Love V, Josephson L, Lichtman AH, Weissleder R. In vivo high resolution three-dimensional imaging of antigen-specific cytotoxic T-lymphocyte trafficking to tumors. *Cancer Res* 2003; 63:6838-46.
- Kelly KA, Allport JR, Tsourkas A, Shinde-Patil VR, Josephson L, Weissleder R. Detection of vascular adhesion molecule-1 expression using a novel multimodal nanoparticle. *Circ Res* 2005; 96:327-36.
- Hulit J, Wang C, Li Z, Albanese C, Rao M, Di Vizio D, Shah S, Byers SW, Mahmood R, Augenlicht LH, Russell R, Pestell RG. *Cyclin D1* genetic heterozygosity regulates colonic epithelial cell differentiation and tumor number in *ApcMin* mice. *Mol Cell Biol* 2004; 24:7598-611.
- Daldrup-Link HE, Meier R, Rudelius M, Piontek G, Piert M, Metz S, Settles M, Uherek C, Wels W, Schlegel J, Rummeny EJ. In vivo tracking of genetically engineered, anti-HER2/neu directed natural killer cells to *HER2/neu* positive mammary tumors with magnetic resonance imaging. *Eur Radiol* 2005; 15:4-13.